Unstable Intermediates. Part CXXXV.[1] The Formation of Sn^{3+} and Pb^{3+} Centres in Irradiated Tin and Lead Salts, and their Electron Spin Resonance Parameters

By **Robert J. Booth, Haydn C. Starkie,** and **Martyn C. R. Symons,*** Department of Chemistry, The University, Leicester LE1 7RH
Raymond S. Eachus, Research Laboratories, Eastman Kodak Company, Rochester, New York 14650, U.S.A.

A wide range of stannous, stannic, plumbous, and plumbic compounds have been exposed to ^{60}Co γ-rays at 77 K and their e.s.r. spectra studied. In most cases very high-field features were detected that can be ascribed to species containing ^{119}Sn, ^{117}Sn, and ^{200}Pb nuclei. These are thought to be Sn^{3+} and Pb^{3+} ions bonded to various ligands characteristic of the host lattices. Trends in the derived hyperfine coupling constants are discussed in terms of environmental effects.

In earlier Parts [2] we reported the unequivocal detection of Cd^+, Hg^+, and Tl^{2+} ions, identification being largely based upon the observation of very high-field features associated with the magnetic isotopes ^{111}Cd, ^{113}Cd, ^{119}Hg, ^{201}Hg, ^{203}Tl, and ^{205}Tl. We found that the isotropic hyperfine coupling constants for these cations were almost independent of environment and concluded that, somewhat surprisingly, the effect of ligand bonding was small.[2] In general, these $-ns^1$ cations were only formed in dilute frozen solution or from the parent ions doped into various host lattices. However, in the particular case of anhydrous cadmium carbonate, Cd^+ ions were detected in the irradiated pure material.[3] This result was thought surprising when considered in terms of simple band-theory, since these monatomic ions cannot distort to provide a well defined localised trap for the excess electron.[3]

During the course of the present search for Sn^{3+} and Pb^{3+} ions,[4] several reports of e.s.r. studies of these species have appeared. Born *et al.*[5] detected Pb^{3+} in irradiated calcium tungstate and in calcium and zinc oxide crystals; Mineeva and Bershov [6] studied Pb^{3+} in irradiated calcium carbonate; Holton and Watts [7] detected Pb^{3+} and Sn^{3+} in irradiated zinc selenide; and Boettcher and Dziescaty [8] detected Sn^{3+} in irradiated cadmium sulphide.

Booth *et al.* incidentally identified a centre formulated as $PbMe^{2+}$ in irradiated plumbous acetate,[9] and Roberts and Eachus [10] identified species described as PbH^+ and Pb^+ in the same material.

EXPERIMENTAL

Salts were either AnalaR or of the highest available purity and were generally used without further purification. Plumbous carbonate was prepared by precipitation from an aqueous solution of the nitrate by addition of aqueous sodium carbonate. The precipitate was washed with water and dried *in vacuo* before irradiation. Plumbous ions were adsorbed on silica gel by a cation-exchange procedure similar to that described by Hathaway and Lewis.[11] Stannous oxide, SnO,xH_2O was prepared by the action of aqueous sodium hydroxide on an excess of aqueous stannous chloride. The precipitated oxide was washed and dried *in vacuo* before use. Stannous acetate and perdeuterioacetate were prepared by the action of boiling glacial acetic acid ($CD_3{\cdot}CO_2D$) on the precipitate formed from the action of aqueous (D_2O) stannous chloride on an excess of aqueous (D_2O) potassium carbonate. The resulting solution gave the acetate as colourless crystals on evaporation. Plumbous acetate and perdeuterioacetate were prepared by the action of freshly precipitated lead carbonate on boiling aqueous (D_2O) acetic acid ($CD_3{\cdot}CO_2D$). The resulting solution was filtered and evaporated and the resulting crystals dried *in vacuo* and recrystallised from either H_2O or D_2O. These samples were irradiated either

[1] Part CXXXIV, Mikhail V. Serdobov and Martyn C. R. Symons, *J.C.S. Perkin II*, 1973, 1808.
[2] R. S. Eachus and M. C. R. Symons, *J. Chem. Soc.* (*A*), 1970, 3080; M. C. R. Symons and J. K. Yandell, *ibid.*, 1971, 760; R. J. Booth, H. C. Starkie, and M. C. R. Symons, *ibid.*, p. 3198.
[3] M. C. R. Symons and R. S. Eachus, *Chem. Comm.*, 1970, 70.
[4] R. J. Booth, H. C. Starkie, and M. C. R. Symons, *J. Phys. Chem.*, 1972, **76**, 141.
[5] G. K. Born, A. Hofstaeter, and A. Scharmann, *Phys. Status Solidi*, 1970, **37**, 255; G. K. Born, A. Hofstaeter, and A. Scharmann, *Z. Phys.*, 1971, **245**, 333; G. K. Born, A. Hofstaeter, and A. Scharmann, *Phys. Letters A*, 1971, **36**, 447.
[6] R. M. Mineeva and L. V. Bershov, *Fiz. Tverd Tela*, 1969, **11**, 803.
[7] W. C. Holton and R. K. Watts, *J. Chem. Phys.*, 1969, **51**, 1615.
[8] R. Boettcher and J. Dziescaty, *Phys. Status Solidi*, 1969, **31**, K71.
[9] R. J. Booth, H. C. Starkie, and M. C. R. Symons, *J.C.S. Faraday II*, 1972, **68**, 638.
[10] H. C. Roberts and R. S. Eachus, *J. Chem. Phys.*, 1972, **57**, 3022.
[11] B. J. Hathaway and C. E. Lewis, *J. Chem. Soc.* (*A*), 1969, 1176.

directly after recrystallisation or after varying periods of vacuum- or air-drying.

Lead tetra-acetate was handled in a dry-box under nitrogen to prevent hydrolysis. Powder samples were sealed in suitable containers and irradiated at 77 K under liquid nitrogen. Solutions were degassed *in vacuo* and immediately frozen as small beads in liquid nitrogen. The beads were transferred to suitable containers which were sealed before irradiation. All irradiations were performed at 77 K in a Vickrad ^{60}Co γ-radiation source, at a nominal dose rate of 4 Mrad h^{-1} for *ca.* 2 h. E.s.r. spectra were measured at 77 K on a Varian E-3 *X*-band spectrometer.

RESULTS AND DISCUSSION

Our main results are summarised together with those of others in Table 1, and typical e.s.r. spectra for the Sn^{3+} and Pb^{3+} centres are given in Figures 1 and 2 (*cf.* Figure 1 of ref. 4). In all cases high-field lines in the 4000—5400 G region were detected, which were assigned to $^{117}Sn^{3+}$, $^{119}Sn^{3+}$, and $^{207}Pb^{3+}$. Sometimes even lines belonging to $^{115}Sn^{3+}$ centres were observed [4] [$^{119}Sn(I = \frac{1}{2})$ 8·68%, $^{117}Sn(I = \frac{1}{2})$ 7·67%, $^{115}Sn(I = \frac{1}{2})$ 0·35%, $^{207}Pb(I = \frac{1}{2})$ 21·1%].

Because of the very large hyperfine coupling constants

TABLE 1

E.s.r. parameters for Sn^{3+} and Pb^{3+} centres in various host lattices and solutions

Host	Species	High-field line positions/G [a]	*g*-values	*A*-values (G) [a] $A_{\parallel}$	$A_{\perp}$	A_{iso}	Ref.
Solid $Pb(ClO_4),3H_2O$	$^{207}Pb^{3+}$	5465 (‖) 5510 (‖)	2·017 ± 0·001	15,500	15,358	15,405	This work
Solid PbF_2	$^{207}Pb^{3+}$	5470 (v. broad line)	2·009 ± 0·001			14,550 ± 200	This work
$CaCO_3$–Pb^{2+}	$^{207}Pb^{3+}$		2·0065 ± 0·005 (‖) 2·0085 ± 0·0005 (⊥)			14,351 ± 5	6
Frozen 2·5M–HNO_3	$^{207}Pb^{3+}$	5500	2			14,052	This work
$CaWO_4$–Pb	$^{207}Pb^{3+}$		1·9919 ± 0·0001 (‖) 1·9887 ± 0·0001 (⊥)			13,720	5
ThO_2–Pb	$^{207}Pb^{3+}$		1·9666 1·9704			13,397 ± 5	
	Pb^{3+}–F^-		1·9649	12,980	12,874		18
CeO_2–Pb	$^{207}Pb^{3+}$		1·9649 ± 0·0008			13·125	18
Solid $PbCO_3$ or $Pb_3(CO_3)_2(OH)_2$	$^{207}Pb^{3+}$	5348	2			12·400	This work
$Pb(OAc)_4$	$^{207}Pb^{3+}$	5432 (‖) 5338 (⊥)	2	12,436 ± 50	12,346 ± 50	12,376	This work
Frozen 4M–$HClO_4$	$^{207}Pb^{3+}$	5570 5370 (v. broad line)	2 2	two different Pb^{3+} sites (i) 15,996 ± 100 (ii) 12,055 ± 500			This work
Frozen 4M–HOAc	$^{207}Pb^{3+}$	5348	2			11,950 ± 10	This work
Silica gel with Pb^{2+} adsorbed	$^{207}Pb^{3+}$	5300	2			11,795 ± 50	This work
KCl–Pb (annealed to 220 K from 77 K)	$^{207}Pb^{3+}$		2·034 ± 0·001			11,592 ± 50	18
CaO–Pb	$^{207}Pb^{3+}$		1·999			11,465	5
$Pb(OAc)_2$	$^{207}Pb^{3+}$	5425 (‖) 5263 (⊥)	2	11,487 ± 50	11,328 ± 50	11,381 ± 50	This work
ZnO–Pb	$^{207}Pb^{3+}$		2·013			8598	5
ZnSe–Pb	$^{207}Pb^{3+}$		2·0729 ± 0·005 2·0721			6457 ± 5 7122 ± 20	7 1
ZnTe–Pb	$^{207}Pb^{3+}$		2·167			5170	18
Solid SnI_2	$^{119}Sn^{3+}$	5255				10·246 ± 50	This work
	$^{117}Sn^{3+}$	5215	2			9733 ± 50	
	$^{115}Sn^{3+}$	Not resolved					
Solid $SnSO_4$	$^{119}Sn^{3+}$	5231 (‖) 5007 (⊥)	2·018 ± 0·001 (‖)	9214	8956	9042	This work
	$^{117}Sn^{3+}$	5186 (‖) 4976 (⊥)		8800	8554	8636	
	$^{115}Sn^{3+}$	5098 (‖) 4916 (⊥)	2·009 ± 0·001 (⊥)	8060	7838	7912	
Solid SnF_2	^{119} $^{117}Sn^{3+}$	*ca.* 500 [c]	2			*ca.* 7896	This work
Solid $Sn(OAc)_2$	$^{119}Sn^{3+}$	5155 (‖) 4862 (⊥)		7554	7229	7337	
	$^{117}Sn^{3+}$	5105 (‖) 4832 (⊥)	2	7216	6909	7011	This work
	$^{115}Sn^{3+}$	5082 (‖) 4810 (⊥)		7026	6718 (± 50)	6821	
Solid $SnCl_2$	^{119} $^{117}Sn^{3+}$	4780 [b]	2			6251	This work
CdS–Sn	$^{119}Sn^{3+}$		2·0024 ± 0·0005 (‖)	5647 ± 5	5436 ± 5	5506·3	8
	$^{117}Sn^{3+}$		2·0031 ± 0·0005(⊥)	5396	5187	5256·7	
ZnSe–Sn	$^{119}Sn^{3+}$		2·0251 ± 0·0004			5042 ± 5	7
	$^{117}Sn^{3+}$		2·0251 ± 0·0004			4819 ± 5	7
SnO,xH_2O	^{119} $^{117}Sn^{3+}$	4370 [b]	2			3470 ± 20	This work

[a] 1 G = 10^{-4}T. [b] Separate isotopic components not resolved. [c] This is the central position of a series of weak, broad lines. A complex ^{19}F superhyperfine pattern on these lines prevented exact resolution into ‖ or ⊥ lines and $^{119}Sn^{3+}$ and $^{117}Sn^{3+}$ isotope lines.

of these centres, in common with many other ns^1,^2S state ions, the expected low-field lines could not be observed at X-band frequencies. Attempts were made

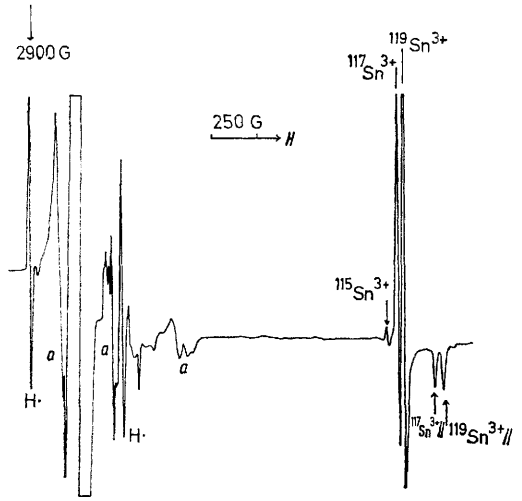

FIGURE 1 First derivative e.s.r. spectrum for stannous sulphate after exposure to ^{60}Co γ-rays at 77 K, showing features assigned to Sn^{3+}. The isotopes responsible for the high-field lines are indicated. The strong central line is assigned in part to this species having non-magnetic isotopes, whilst the remaining features (*a*) are as yet unidentified

to observe them by use of a Q-band spectrometer,[12] but to no avail, probably because of the lack of stability of the Q-band magnet at very low fields.

Generally, approximate hyperfine coupling constants were calculated from the measured high field lines on the reasonable assumption that $g = ca.\ 2{\cdot}0$ for these centres. Although both tin and lead have non-magnetic

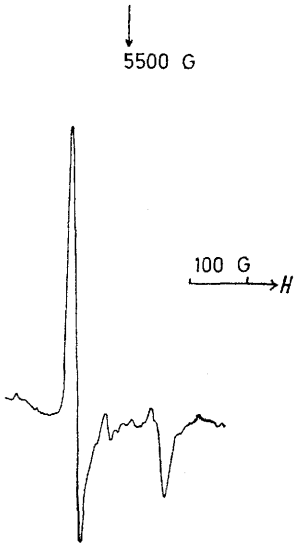

FIGURE 2 First derivative e.s.r. spectrum for lead perchlorate after exposure to ^{60}Co γ-rays at 77 K, showing features assigned to Pb^{3+} ions containing ^{207}Pb

nuclei, the e.s.r. lines for Sn^{3+} and Pb^{3+} species containing them could only be positively identified in a few cases, because of the presence of other intense absorptions in the free-spin region. When such central lines were established, accurate g and A-values for the M^{3+} centres could be calculated. The method used to calculate the A-values for these centres is described in the Appendix, since the normal Breit–Rabi equation[13] can only be used for species with an isotropic hyperfine coupling constant. The calculated results are shown in Table 1. The isotropic hyperfine coupling constants tend to increase as the ionic character of the host lattice increases. Thus, in contrast with our results for Cd^+, Hg^+, and Tl^{2+} the metal–ligand bonding now has a significant effect upon the orbital of the unpaired electron.

This is illustrated in Figure 3 where A_{iso} is plotted against the partial ionic character of the A–B bond where AB is the host lattice. The latter was calculated

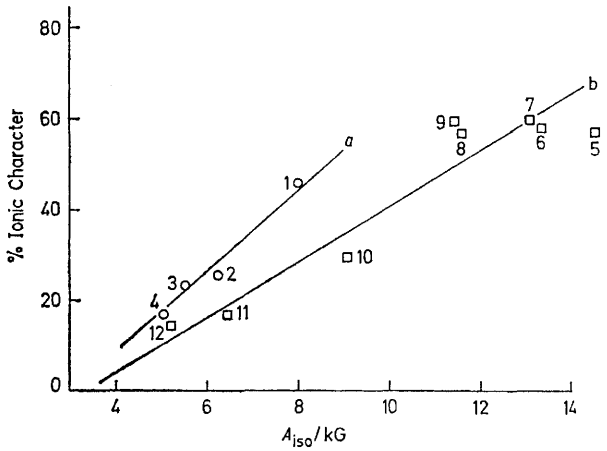

FIGURE 3 Trends in A_{iso} for (*a*) Sn^{3+} and (*b*) Pb^{3+} isotropic hyperfine coupling constants with % ionic character of the host lattices: 1, SnF_2; 2, $SnCl_2$; 3, CdS–Sn; 4, ZnSe–Sn; 5, PbF_2; 6, ThO_2–Pb; 7, CeO_2–Pb; 8, KCl–Pb; 9, CaO–Pb; 10, ZnO–Pb; 11, ZnSe–Pb; and 12, ZnTe–Pb

from the electronegativities of the A (χ_A) and B (χ_B) groups, by use of formula (1).[14]

$$\%\ \text{Ionic character} = 16|\chi_A - \chi_B| + 3{\cdot}5|\chi_A - \chi_B|^2 \quad (1)$$

The anions clearly play a major role; the more ionic the M^{3+}–anion bond, the more the unpaired electron is localised in the pure *ns* atomic orbital. The role of the host lattice cations must then be to modify the donicity of these ligands; the stronger the bonding to the host cations the weaker the bonding to the paramagnetic M^{3+} centres.

The crudity of the values used in Figure 3 being considered, the result is satisfactory, especially for Pb^{3+}. The relatively poor correlation for Sn^{3+} arises largely from the inaccuracy in measurement of the high-field line positions of this species in stannous oxide, fluoride, and iodide samples since these lines were always broad and of low intensity.

The other major aspect of our results is the remarkable

[12] J. A. Brivati, J. M. Gross, M. C. R. Symons, and D. J. A. Tinling, *J. Chem. Soc.*, 1965, 6504.

[13] G. Breit and I. Rabi, *Phys. Rev.*, 1931, **38**, 2082.

[14] N. B. Hannay and C. P. Smyth, *J. Amer. Chem. Soc.*, 1946, **68**, 171.

stability of the Sn^{3+} and Pb^{3+} centres in many stannous and plumbous salts. As stressed previously,[3,4] this is at first surprising. However, the key to understanding why this should be probably lies in the large sensitivity of the A_{iso} values to the nature of the host lattice. Thus in the parent salts, the Sn^{2+} and Pb^{2+} ions are weakly bonded to neighbouring anions, but this bonding is considerably strengthened for the new M^{3+} centres because of the greater positive charge. Equally, the loss of one of the outer *s*-orbital electrons makes this orbital partially available for bonding to the ligands. This increase in bonding makes the centre thermodynamically more stable than any alternative centre formed by electron donation from neighbouring Sn^{2+} ions, unless considerable ligand relaxation occurs during the transfer process.

rhombic) systems is to determine the roots of the axial spin hamiltonian for the system.[16,17] On application of the selection rules and resonance condition to these equations, and taking $g_{\parallel} \sim g_{\perp} \sim 2{\cdot}0$, expressions (3) and (4) are obtained where

$$H_{0\parallel} = \tfrac{1}{2}A_{\parallel} + \tfrac{1}{4}\{2H_{1\parallel} + (4H_{1\parallel}^2 + 4A_{\perp}^2)^{\frac{1}{2}}\}$$
$$= -\tfrac{1}{2}A_{\parallel} + \tfrac{1}{4}[2H_{2\parallel} + (4H_{2\parallel} + 4A_{\perp}^2]^{\frac{1}{2}} \quad (3)$$

$$H_{0\perp} = \tfrac{1}{2}A_{\perp} + \tfrac{1}{4}\{[4H_{1\perp}^2 + (A_{\parallel} - A_{\perp})^2]^{\frac{1}{2}} + [4H_{1\perp}^2 + (A_{\parallel} - A_{\perp})^2]^{\frac{1}{2}}\}$$
$$= -\tfrac{1}{2}A_{\perp} + \tfrac{1}{4}\{[4H_{2\perp}^2 + (A_{\parallel} - A_{\perp})^2]^{\frac{1}{2}} + [4H_{2\perp}^2 + (A_{\parallel} - A_{\perp})^2]^{\frac{1}{2}}\} \quad (4)$$

Equations (3) and (4) were solved from the $H_{0\parallel}$ and $H_{\perp 0}$, $H_{2\parallel}$, and $H_{2\perp}$ values by the use of a computer programme which used the measured or estimated $H_{0\parallel}$ and $H_{0\perp}$ and guessed values of $A_{\parallel}$ and $A_{\perp}$. By iterative use of equations (3) and (4) these guessed *A*-values were refined until self-consistent.

TABLE 2

The effect of calculating large hyperfine coupling constants by use of the Breit–Rabi equation and the roots of the spin Hamiltonian for an axial system

Species	Breit–Rabi		Axial (see Appendix)	
	A-value/G	*g*-value	*A*-value/G	*g*-value
$^{207}PbMe^{2+}$	1928 ± 20 (∥)	1·953 ± 0·002 (∥)	1962 ± 20 (∥)	1·994 ± 0·002 (∥)
(Anhydrous)	1700 ± 20 (⊥)	1·988 ± 0·002 (⊥)	1689 ± 20 (⊥)	1·968 ± 0·002 (⊥)
$^{119}Sn^{3+}$ in $SnSO_4$	11,354 ± 10 (∥)	2·018 ± 0·001 (∥)	9214 ± 10 (∥)	2·018 ± 0·001 (∥)
$SnSO_4$	8246 ± 10 (⊥)	2·009 ± 0·001 (⊥)	8956 ± 10 (⊥)	2·009 ± 0·001 (⊥)

The above Table shows the dangers of calculating the e.s.r. parameters for axial spin systems by using the Breit–Rabi equation. In the case of the $^{207}PbMe^{2+}$, the *A*-values calculated by the two methods agree within experimental error, which fortunately means that the model for the structure and bonding in this species, which was based on Breit–Rabi corrected *A*-values, is still valid. However, by the axial method, we get $g_{\parallel} > g_{\perp}$, which was what we would have expected from our models of the electronic structure of this radical. The original Breit–Rabi result of $g_{\parallel} < g_{\perp}$ was very difficult to explain on this model. The central ⊥ lines of this species would still be observed in the same position of the spectrum, but the ∥ lines would be obscured by the Me and other species in the $g = 2$ region of the spectrum. Hence our ability to observe the diamagnetic nuclear $PbMe^{2+}$ ⊥ lines in our spectra but not the ∥ lines.

In the case of the $^{114}Sn^{3+}$, the Breit-Rabi equation gave a very large $2B$ value for this species, far in excess of the calculated $2B^{\circ}$ value. After correction by the axial method, the $2B$ value is very reasonable. This explains why, in our original report on the M^{3+} centres, very enhanced anisotropies, which at the time we could not explain, were observed. The Breit-Rabi equation had also been used to correct these hyperfine values originally.

In several cases, hyperfine anisotropy was detected (Table 1) but we feel that the inaccuracy of the data is such that quantitative comparisons are not warranted. Our new procedure for estimating these values (Appendix has, however, removed the difficulty previously experienced, in which the apparent anisotropy was greater than that estimated for complete occupancy of an outer *p*-orbital.[4]

APPENDIX

Calculation of Hyperfine Coupling Constants.—In all the systems discussed in this paper the simple spin hamiltonian (2) applied. If the *g* and *A* tensors are

$$H = g\beta \mathrm{H} \cdot \mathrm{S} + \mathrm{I} \cdot A \cdot \mathrm{S} - g_{\mathrm{N}}\beta_{\mathrm{N}}\mathrm{H} \cdot \mathrm{I} \quad (2)$$

isotropic, then the roots of this hamiltonian give the Breit–Rabi [13,15] equation. However, if this method is applied to non-isotropic systems, the calculated values of *A* will be in error. This is illustrated in Table 2.

The method which should be used to treat axial (or

This simple programme was checked against the far more complete programme FIELDS.[18] The results were found to be in excellent agreement. However, our programme can only be used for $I = \frac{1}{2}$ systems, whilst FIELDS is suitable for any spin system.

Table 2 also gives results for the $PbMe^{2+}$ species previously described.[9] We previously used the Breit–Rabi equation to estimate the parameters for this species, and although the resulting *A*-values were satisfactory the *g*-values were not. We had been unable to explain the low value for $g_{\parallel}$, since our model for this species required $g_{\parallel} = ca.\ 2$. This requirement is now seen to be satisfied (Table 2).

We thank the S.R.C. for grants (to R. J. B. and H. C. S.).

[3/843 *Received*, 19*th April*, 1973]

[15] J. E. Nafe and E. B. Nelson, *Phys. Rev.*, 1948, **73**, 718.
[16] P. W. Atkins and M. C. R. Symons, 'The Structure of Inorganic Radicals,' Elsevier, Amsterdam, 1967.
[17] C. R. Byfleet, D. P. Chong, J. A. Hebden, and C. A. McDowell, *J. Magnetic Resonance*, 1970, **2**, 69.
[18] J. L. Kolopus, C. B. Finch, and U. U. Abraham, *Phys. Rev.*, 1970, *B*, 12, 2040; D. Shoemaker and J. L. Kolopus, *Solid State Comm.*, 1970, 8, 435; Ken Suto and Masaharu Aoki, *J. Phys. Soc. Japan*, 1969, **26**, 287; Ken Suto and Masaharu Aoki, *ibid.*, 1967, **22**, 1307.